


 Cite this: *RSC Adv.*, 2026, 16, 7022

Nanobiocatalytic upgrading of heavy oil using *Geobacillus stearothermophilus* and alumina nanoparticles

 Ali Maghzi,^a Arezou Jafari,^b Seyyed Mohammad Mousavi^{b,c} and Riyaz Kharrat^d

Challenges in heavy oil biougrading necessitate innovative approaches. Hence, we delved into the simultaneous application of a bacterium (*Geobacillus stearothermophilus*) and Al₂O₃ nanoparticles for heavy oil upgrading at a high temperature. We used the central composite design method within Design Expert software. The initial oil volume, upgrading time, and nanoparticle concentration were the main variables. Aromatic/aliphatic content and oil viscosity were the two independent responses. Results showed that nanoparticles could have accelerated biougrading. The zeta potential, FESEM and EDS confirmed the absorption of nano alumina on the bacterial cell due to the formed ion–dipole interaction between alumina and bacterial cells, which could have intensified the entry of heavy oil molecules into the bacterial cell. The best outcomes were observed during 11.86 days, with 26% v/v initial oil and 0.46% W nanoparticles, as indicated by FTIR spectroscopy, which showed a reduction in the aromatic/aliphatic index from 0.29613 to 0.07677 and a decrease in oil viscosity from 480 cp to 144 cp. Moreover, as determined by GC-MS, a remarkable 100% decrease in certain cyclo compounds and a considerable improvement in upgrading efficiencies for some contents such as cyclohexanes were observed. Also, a 14% decrease in asphaltene content was associated with a decrease in the solo use of bacteria. These findings highlight the synergistic efficacy of *G. stearothermophilus* and alumina in upgrading heavy oil.

 Received 11th October 2025
 Accepted 21st December 2025

DOI: 10.1039/d5ra07786a

rsc.li/rsc-advances

Introduction

The main objective of “biougrading” is to include all: (i) activities that make the material easier to produce and transport; (ii) chemical changes that increase the value of the oil while reducing severe environmental impacts. Different reactions that could change the properties of heavy crude oil are included, but not limited to, cutting internal linkages of heavy molecules such as asphaltenes, aromatics, and resins.¹

The degradation of asphaltenes into lighter fragments by microorganisms is considered a key activity in biougrading.² Species of *Alcanivorax*, *Marinobacter*, *Thalassolituus*, *Cycloclasticus*, and *Oleispira* have been identified as key organisms with major roles in the degradation of petroleum hydrocarbons for cleaning up marine oil spills.³ Some studies have shown that bacteria of the species *Raoultella*, *Ochrobactrum*, and *Serratia* can reduce the resin content of the heavy fraction of the refinery distillation column, while increasing aliphatic and aromatic contents.⁴ One study showed that the amount of saturates

increased, while the amounts of resins decreased, when using native microbial consortia from oil-polluted soil samples.⁵ Laboratory research on the effect of bacteria on asphaltene degradation showed that *Pseudomonas* species and *Bacillus* species could degrade asphaltene molecules of heavy oil up to 28 °C during the 2 months of upgrading.⁶ *Pseudomonas* species played a key part in heavy oil upgrading, especially in desulfurization. In this regard, one study showed sulfur removal from bituminous coal at 30 °C over 60 h, with a maximum desulfurization rate of 40.6%.⁷ The ability of microorganisms to upgrade heavy oil at high temperatures is also highly favorable for the application of such bacteria in oil reservoirs. Results of a study on the effect of *Geobacillus stearothermophilus* on upgrading oil molecules showed a considerable reduction in oil viscosity.⁸ Research on the effect of *G. stearothermophilus* on the stability of paraffin wax in crude oil structure showed that microorganisms can use crude oil, thereby creating favorable wettability and degrading residual oil.⁹ A study of the adaptability of microorganisms as a key parameter in biougrading in a hydrocarbon environment containing normal alkanes has shown that adaptability occurred later for C20+ than for lighter molecules.¹⁰ In environmental research on hydrocarbon contamination due to the co-presence of a chemical mixture, results showed that their removal from the environment cannot rely on a single species alone.¹¹ Investigation of the effect of *Enterobacter cloacae* and *Pseudomonas aeruginosa* on the

^aPetroleum Engineering Department, Chemical Engineering Faculty, Tarbiat Modares University, Tehran, Iran. E-mail: ajafari@modares.ac.ir
^bBiotechnology Department, Chemical Engineering Faculty, Tarbiat Modares University, Tehran, Iran. E-mail: mousavi_m@modares.ac.ir
^cModares Environmental Research Institute, Tarbiat Modares University, Tehran, Iran

^dGeoenergy Department, Montanuniversität, Leoben, Austria


degradation of asphaltene molecules showed a strong dependence on upgrading phenomena for the wettability of bacterial cell surfaces. Results of studies on cell wettability alteration by surfactants showed that surfactants rendered the cell surface hydrophobic, thereby improving the degradation of asphaltene.¹² One study investigated the effect of *Enterobacter cloacae* and *Acinetobacter calcoaceticus* for biosurfactant production as a key metabolite for enhanced oil recovery and reported that *Enterobacter* species increased oil recovery by up to 67%.¹³ One study focused on enriching several bacterial consortia from oilfield samples. Results revealed up to a 127% increase in saturates, a 54% decrease in aromatics, 52% decrease in asphaltene, and 87% increase in resins.¹⁴ Some scholars have investigated other heavy oil recovery and upgrading methods. Zhang¹⁵ studied a steam flow model for a horizontal wellbore in the SAGD process. Results showed that in the area between horizontal well patterns, the temperature rise was not obvious, and most of the heat energy was recovered after a long period of steam injection. Scholars have investigated the catalytic performance in upgrading heavy oil by synthesizing active microemulsion catalysts¹⁶ and by using a novel nanocomposite catalyst for aquathermolysis.¹⁷ Results showed that the rate-controlling step in light hydrocarbon production was no longer operative when the temperature increased from 70 °C to 90 °C. Furthermore, recent research has demonstrated the application of nanostructures, such as nanosheets, to improve heavy oil quality.¹⁸ However, applying microorganism metabolites in heavy oil upgrading has been the center of attention. Recently, scholars investigated the synergetic effect of synthetic nanosilver particles and microbial surfactants in the enhancement of crude oil recovery, and results showed a final increment of 19.49% in oil recovery.¹⁹

Recent studies have shown that nanotechnology could help biotechnology in heavy oil biougrading. Adsorption of alumina nanoparticles onto bacterial cells could improve biodesulfurization, a key mechanism in biougrading,^{20,21} besides other applications of nanostructures in heavy oil upgrading.^{22,23} Biosorption, as one of the key mechanisms in the absorption of heavy metal oxide pollutants from the environment, has recently emerged as a synergetic field of biotechnology and nanotechnology.^{24,25} The development of such synergy has increased in recent years; for example, the application of *Shewanella oneidensis* MR-1 cells led to high efficiency in removing metal pollutants at the nanoscale over 24 h.²⁶

Other studies have shown the coupled effect of silver (Ag), iron oxide (Fe₃O₄), and alumina nanoparticles, and their interactions if incorporated into a collagen (C)-based nanobiocomposite (NBC). Results showed that an NBC from biowaste provided enhanced antibacterial effects and reinforcement for biological applications.^{27–29} Another study evaluated the coupled effect of CuO nanorods with soy protein, which, due to its enhanced thermal stability, was considered an eco-friendly and cost-effective NBC for industrial and pharmaceutical applications.³⁰ However, the solo function of nanotechnology in removing pollutants by developing cracking and absorption mechanisms has been a trend.^{31–34} Studies have shown that nanostructures such as nano alumina and iron

oxide, which are not toxic to microorganisms, can facilitate the bacterial metabolism of heavy oil molecules. However, no study has examined the simultaneous effect of *G. stearothermophilus* bacteria and Al₂O₃ nanoparticles on upgrading heavy oil under reservoir conditions.³⁵

This work presents, for the first time, novel nanobiougrading at higher temperatures. The literature mainly refers to the potential of other bacteria and only at ambient temperatures. Furthermore, studies have focused on nanobiodesulfurization without quantitatively analyzing the chemical changes of heavy oil molecules. Nevertheless, no comprehensive analysis has been conducted using a combined qualitative and quantitative approach to examine the structural changes in the composition of heavy crude oil resulting from nanobiougrading by *G. stearothermophilus* and Al₂O₃ nanoparticles. Hence, we studied the impact of simultaneous use of *G. stearothermophilus* bacteria and Al₂O₃ nanoparticles in the structural upgrading of heavy crude oil under reservoir conditions. We did this to minimize environmental apprehensions and to enhance crude oil value before exposure of its hazardous components to the environment, which has not been studied before.

Materials and methods

Materials

Nutrient broth (NB) and nutrient agar (NA) from Merck were used as the growth media for bacteria. Asphaltenic heavy crude oil (20 API) was collected from one of the heavy oil fields in Iran. It contained 0.24% W of nitrogen and 4.29% W sulfur content. The original SARA test showed 47.9% saturates, 28.10% aromatics, 14.9% resins, and 9.10% asphaltenes. A control laboratory experiment was run under the same experimental conditions, without any microorganism solution, by keeping the original crude oil in a shaker incubator at 60 °C to distinguish biological from abiotic effects on crude oil upgrading. *G. stearothermophilus* strain (PTCC number 1713) was purchased from the Iranian Research Organization for Science and

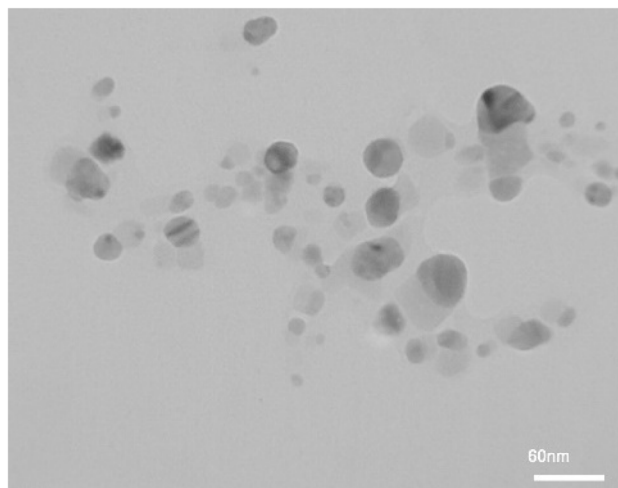


Fig. 1 TEM for applied alumina nanoparticles.



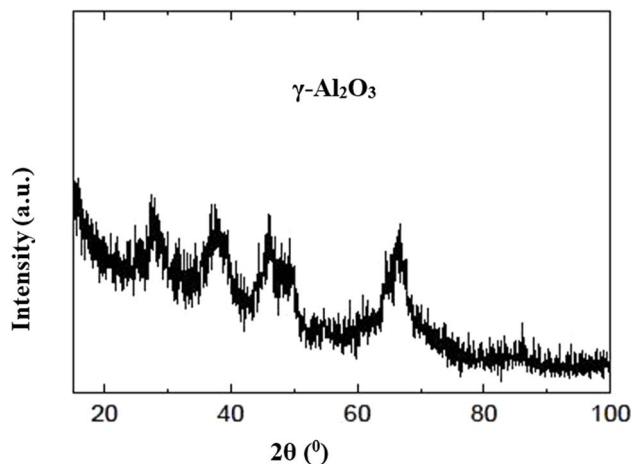


Fig. 2 XRD analysis for applied alumina nanoparticles.

Technology. Al_2O_3 nanoparticles (average particle size: 20–30 nm) were purchased from Nano-Sani and used as the nano-structured material in this research. Fig. 1 and 2 show the TEM and XRD analyses for alumina nanoparticles, respectively.

Methods

The genus *Geobacillus* was created by Nazina *et al.* in 2001 based on *Bacillus* (now *Geobacillus*) *stearothermophilus* DSM22 as the type strain. Other additions followed, and most of these species had an optimum growth range at 55–65 °C. These bacteria can maintain membrane fluidity at high temperatures and form heat-resistant spore-forming biofilms. They usually utilize carbon for heterotrophic/autotrophic growth.³⁶ Hence, such characteristics have made them excellent choices for hydrocarbon upgrading in environmentally harsh conditions.

Samples were placed in an autoclave at 120 °C for 15 min before adding oils to remove potential contamination and microorganisms from the nutrient medium. For all upgrading experiments, bottles were placed in a shaker incubator for the specified upgrading times. Although *G. stearothermophilus* is a facultative bacterial strain, in this research, the shaker rotation was set to 140 rpm under aerobic conditions to achieve acceptable aeration. *G. stearothermophilus* was selected to enrich the novelty of our research but also for its abilities. The first precautionary preparations, such as monitoring the growth of purchased *G. stearothermophilus* on NA plates, were performed in an incubator at 60 °C to ensure there were no pollutants from the original bacterial environment. Furthermore, to conclude the logarithmic growth curve of the bacterium for subsequent inoculation runs, the optical density at 600 nm (OD_{600}) of nutrient media containing *G. stearothermophilus* was recorded by a spectrophotometer to obtain the growth curve of the bacteria. This growth curve was considered for all inoculation runs. Also, in all tests, oil was added to samples at the logarithmic phase of the growth curve. Incubations were run at a fixed environmental condition of 60 °C upon 140-rpm aeration. Time was considered the key variable in upgrading experiments. The other variable parameters in the

Table 1 Table generated through the CCD method

Run	Oil content (%V)	Time (day)	Nanoparticle content (%W)
1	17	9	0.4
2	17	23	0.4
3	23	9	0.4
4	20	16	0.5
5	14	16	0.3
6	23	23	0.4
7	23	9	0.2
8	20	16	0.3
9	23	23	0.2
10	20	30	0.3
11	20	16	0.3
12	26	16	0.3
13	20	16	0.3
14	20	2	0.3
15	17	9	0.2
16	20	16	0.1
17	17	23	0.2
18	20	16	0.3

experiment were the initial oil volume percent and the nanoparticle concentration. Two key measured responses were considered based on the experimental design: ratio of aromatic : aliphatic content index and oil viscosity. Due to the novelty and importance of unifying the experiment temperature with the reservoir temperature, and the importance of the adaptability of bacteria to the real environmental conditions of the oil reservoir, the upgrading test temperature was fixed at 60 °C. Other environmental conditions, such as aerobic/anaerobic states and shaker aeration rates, were fixed to eliminate any extra effect upon test results. In line with the planned research, as well as pilot and field scales, heavy oil was sourced from one of the heavy oil fields in Iran. Based on the considered levels of variables, the designated experimental table (Table 1) for the central composite design (CCD) methodology in Design Expert software, containing 18 runs, was followed.

Preparation of samples

First, 18 runs of Erlenmeyer flask-containing NB media were done. Then, nanoparticles were dispersed using an ultrasonic probe in 18 sets of pre-sterilized Erlenmeyer flasks containing NB media. Then, the inoculation was run by 10% inoculation from the base Erlenmeyer flask into each Erlenmeyer flask. Before inoculating 10% into 18 Erlenmeyer flasks, the bacterial count was run; the colony count was 150–200 CFU per mL. After 10% inoculation into each of 18 Erlenmeyer flasks, the counting was repeated, and the results were in the order of 150 CFU per mL. Finally, oil was added to the Erlenmeyer flasks as detailed in Table 1, and the flasks were placed at 60 °C in a shaker incubator.

Extraction of upgraded oil

Upgraded oil samples were separated from the bacterial medium using filter paper after the specified upgrading time, as shown in Table 1.



Analyzing the oil

We analyzed the original and upgraded samples using qualitative and quantitative methods. (i) Qualitative analysis through viscosity measurement, Fourier transform infrared (FTIR) spectroscopy, gas chromatography-mass spectrometry (GC-MS), and field emission scanning electron microscopy (FESEM); (ii) quantitative analysis using mass analyses and nanobiougrading efficiency (NBUE) analyses. A control laboratory experiment was run in the same experimental condition without any microorganism solution separately at the optimum point. This was done by running the tests in the presence of nanoparticles and bacteria to distinguish the biological effect and nanoparticle effect on crude oil upgrading. Then, FTIR spectroscopy, GC-MS and viscosity measurement were done.

Viscosity

Viscosity measurements were performed in accordance with the details in Table 1 to analyse the effect of the range of variables on upgrading using the Brookfield rotational rheometer (USA). Based on predefined experiments, for each run, the Erlenmeyer flask was removed from the shaker incubator and, hence, the viscosity measurement was conducted at the ambient temperature.

Mass analysis

The upgrading of crude oil was quantified using mass analysis. The crude oil present in the fermentation broth was extracted using filter paper. The concept of the mass analysis method originates from the quantitative method, which has been shown (by Rehman *et al.*³⁷) to provide quantitative measurement of oil degradation percentage. The extraction was repeated twice to completely remove crude oil from the bacterial solution. Then, quantitative upgrading was estimated by dividing the weight of the upgraded oil sample by that of the original oil sample.

FTIR spectroscopy

FTIR spectroscopy was used to analyze the variation in functional groups between the original crude oil and upgraded oils. Tests were run on an FTIR spectrometer (Thermo Scientific, USA). Results were presented as spectra with peaks between 400 and 4000 cm^{-1} , at a resolution of 1 cm^{-1} . The peaks of the original crude oil and those of upgraded oils after different upgrading times were compared. To quantitatively analyze upgrading of crude oil in terms of key fractions such as aliphatics and aromatics, some indices were defined, and FTIR spectra were analyzed.

GC-MS

We ran a GC-MS instrument using a stainless-steel column of dimensions 31 × 16 × 28 cm (6890N/NSD:5973; Agilent Technologies, USA). The SimDis system was used as the GC-MS solution software. Our novel method also calculated NBUE. High-temperature-gas chromatography (HT-GC) with toluene as the solution was applied using a high-temperature GC metal column because most of the fractions fall within the range of

C40–C60 with boiling points in the range 500 to 800+ °C. The device was engineered to withstand such high temperatures.

The mass selective detector (MSD) we used combined the separation power of GC with the mass analysis capabilities of a mass spectrometer. A fast-heating oven with 240 V/15 A power was employed. The power cord was rated for 250 V/15 A and was a two-pole, three-wire cord with grounding (type L6-15R/L6-15P). The injection temperature was 50 °C to 450 °C.

NBUE

In the quantitative analysis of GC-MS data, some key aliphatic and aromatic molecules were focused upon to find the nanobiougrading capability of *G. stearothermophilus*.³⁸ They could be measured by the NBUE index for each component, which is the weight of the component in the upgraded oil divided by its weight in the original oil. The weight of each component was extracted from GC-MS results.

FESEM

FESEM was performed to confirm the morphology and bacilli shape of *G. stearothermophilus*. Also, the decoration of *G. stearothermophilus* bacteria with nanoparticles was shown.

EDAX

To confirm the purity and distribution of constituents in the nanobacterial solution, an EDAX test was performed on the final nanobiosolution containing *G. stearothermophilus* and alumina nanoparticles, prepared at the optimal nanoparticle concentration (0.46% W). The EDAX test was supported by FESEM to depict the true cell permeability.

Zeta potential

To support the FESEM observation on the bacterial decoration by nanoparticles, zeta potential measurement and supplementary FESEM at the optimum nanoparticle concentration (0.46% W) were run to prove the surface charge of nanoparticles.

Results and discussion

We investigated the nanobiougrading potential of the simultaneous use of *G. stearothermophilus* bacteria and alumina nanoparticles under predefined environmental conditions. The test temperature was set at 60 °C. The experiment was run under aerobic conditions, with the shaker incubator aeration set to 140 rpm during different upgrading time intervals. The different levels of crude oil quantities and nanoparticle concentration were maintained as per Table 1. To analyze the nanobiougrading process, FTIR spectroscopy and GC-MS were performed to investigate the results quantitatively and in line with qualitative analysis.

Mass analysis

The quantitative upgrading of crude oil was determined by mass analysis. Crude oil weight was measured before and after upgrading at different upgrading times, and the initial oil



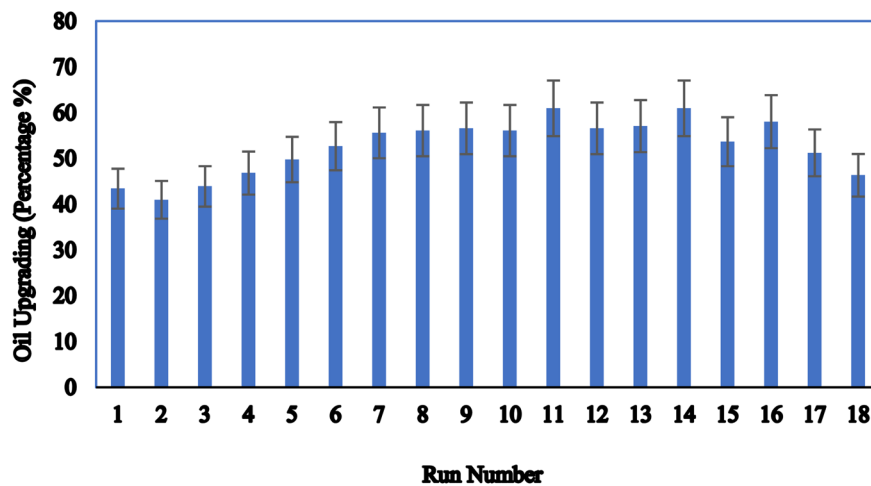


Fig. 3 Upgrading percentage for 18 experiment runs using the mass method.

volume and nanoparticle concentrations were measured. The upgrading percentage was calculated. The results are shown in Fig. 3. According to the results, the upgrade was delayed by up to 12 days. After 12 days, the slope of the curve was relatively smooth. This may have been due to nutrient consumption in the media. After 28 days, as soon as the bacteria fully adapted to the crude oil medium and began using oil molecules as a monoenergetic source, the upgrading process began to speed up. According to the experimental design based on the 18 designated runs in Table 1, the software generated four identical center points to emphasize the reproducibility. In this step, the run numbers 8, 11, 13, and 18 had the same condition and were designed solely to check and confirm reproducibility. The results of these runs confirmed that the measurements were in the same range.

FTIR spectroscopy for upgraded oils

FTIR spectroscopy was used to analyze the variation in functional groups between the original crude oil and upgraded oils. Two major indices were defined to quantitatively analyze the upgrading of crude oils in terms of key compounds.³⁸ The results of the analysis are shown in Table 2. Aligned with the FTIR spectra shown in Table 2 for 18 runs shown in Table 1, aliphatic molecules at 2953–2954 cm^{-1} were not present in the original crude oil, and were formed and detected in the upgraded oil after 12 days of upgrading. This may have been due to the cleavage of carbon–carbon double bonds in the range 1904 cm^{-1} and aromatics in the range 862 cm^{-1} , which disappeared after 12 days of upgrading. However, the other aliphatic peaks at 2927.23, 2855.54, 1462.87 and 1377.00 cm^{-1} in the original oil varied during the upgrading process. As shown in Table 2, the aromaticity index for the original crude oil was 0.1678, which increased to 0.2439 after 2 days and then decreased to 0.0640 after 9 days of upgrading with 0.4% W nanoparticles. The first jump may have been due to the unpredictable but favorable behavior of bacteria. This decrease for up to 9 days was a desirable achievement. Due to the importance of the ratio of aromatic : aliphatic contents, the ratio of indices was considered as a key response for optimizing results. As with the aliphatic index, the aromatic analysis did not rely solely on the 862 cm^{-1} peak. Peaks at 744.29, 810.37, 862.80 and 1573.59 cm^{-1} were considered as aromatic peaks and involved in index calculation.

However, the discrepancy after 9 days may reflect the unpredictable behavior of bacteria in selecting hydrocarbon molecules for their metabolism. The same behavior was shown for the aliphatic index.

FESEM

FESEM was performed to confirm the morphology and bacilli shape of *G. stearothermophilus*, as well as the decoration of nanoparticles on the cell surface. The results are shown in Fig. 4–7. The rod shape of *Bacillus* species could be detected by

Table 2 FTIR spectroscopy of crude oil alteration during upgrading for 18 runs

Run	Aromaticity index	Aliphatic index
Original crude oil	0.1678	0.7236
Run 01	0.0640	0.8334
Run 02	0.1632	0.7344
Run 03	0.2310	0.3461
Run 04	0.1990	0.2710
Run 05	0.5225	0.1721
Run 06	0.5027	0.0437
Run 07	0.4071	0.2976
Run 08	0.2071	0.3679
Run 09	0.5106	0.0567
Run 10	0.2498	0.0413
Run 11	0.4494	0.1674
Run 12	0.3190	0.2558
Run 13	0.1391	0.0195
Run 14	0.2439	0.4127
Run 15	0.2657	0.2964
Run 16	0.3208	0.0113
Run 17	0.0628	0.2036
Run 18	0.3643	0.4057



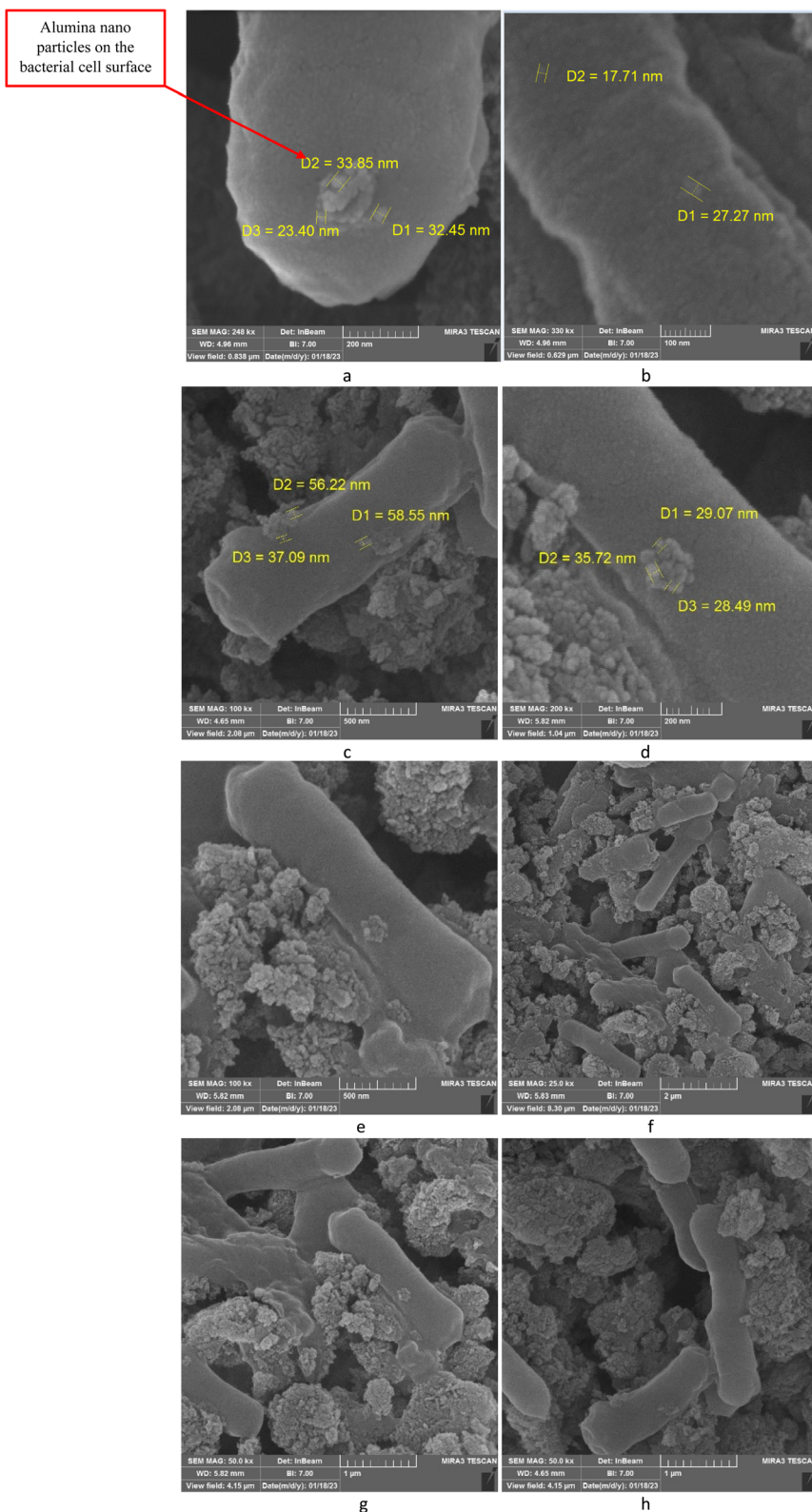


Fig. 4 FESEM of *G. stearothermophilus* decorated with alumina nanoparticles at 0.1% W concentration with magnifications of (a) 200 nm, (b) 100 nm, (c) 500 nm, (d) 200 nm and bacterial cell situation with magnifications of (e) 500 nm, (f) 2 µm, (g) and (h) 1 µm.

FESEM. Also, the decoration was better than the others at the highest nanoparticle concentration. Fig. 4a and b depict the nanoparticle decoration on bacterial cells at magnifications of

200 nm and 100 nm, respectively. Fig. 4c–f show the situation of bacterial cells at different magnification scales. Fig. 4g and h depict the nanoparticle decoration at magnifications of 500 nm



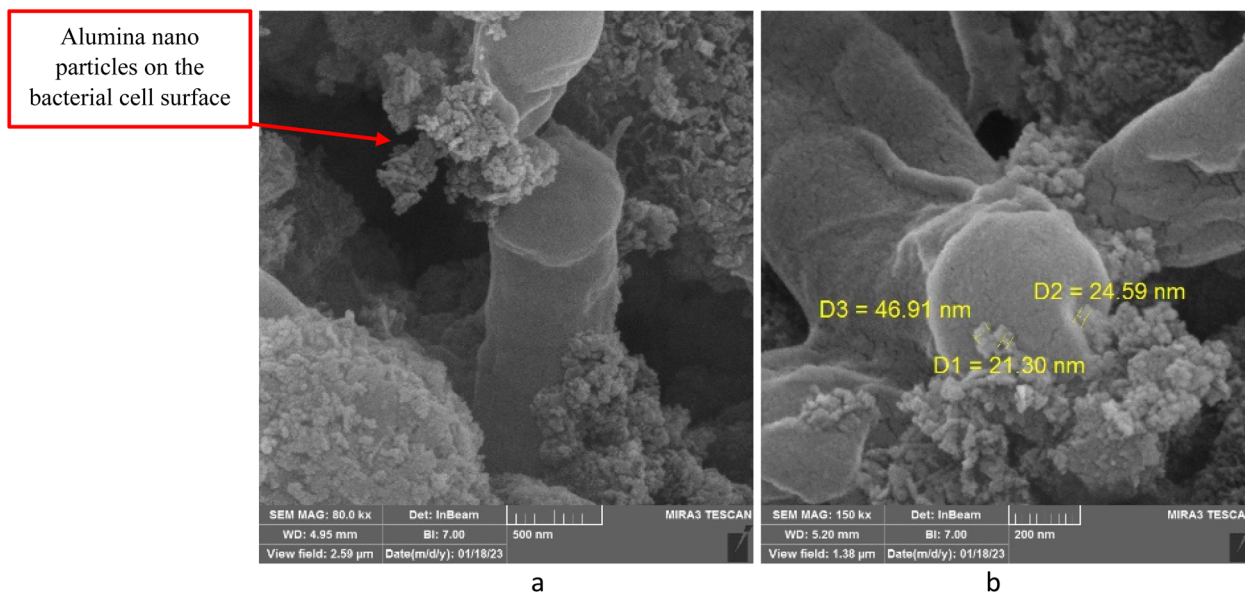


Fig. 5 FESEM of *G. stearothermophilus* decorated with alumina nanoparticles at 0.3% W concentration for magnifications of (a) 500 nm and (b) 200 nm.

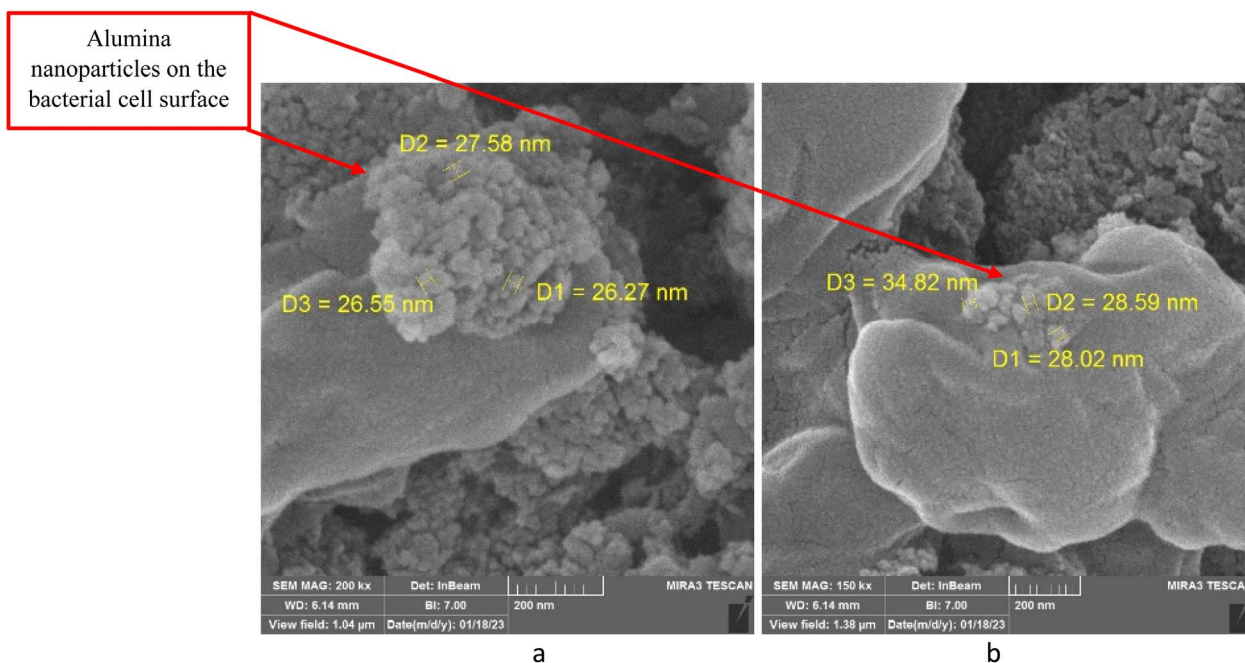


Fig. 6 FESEM of *G. stearothermophilus* decorated with alumina nanoparticles at 0.5% W concentration showing (a) agglomeration of particles and (b) fully dispersed nanoparticles.

and 200 nm, respectively. Fig. 5 shows *G. stearothermophilus* decorated with alumina nanoparticles at 0.3% W concentration with different magnification scales. Fig. 6 depicts such decoration with alumina nanoparticles with 0.5% W concentration with different magnification scales.

EDAX

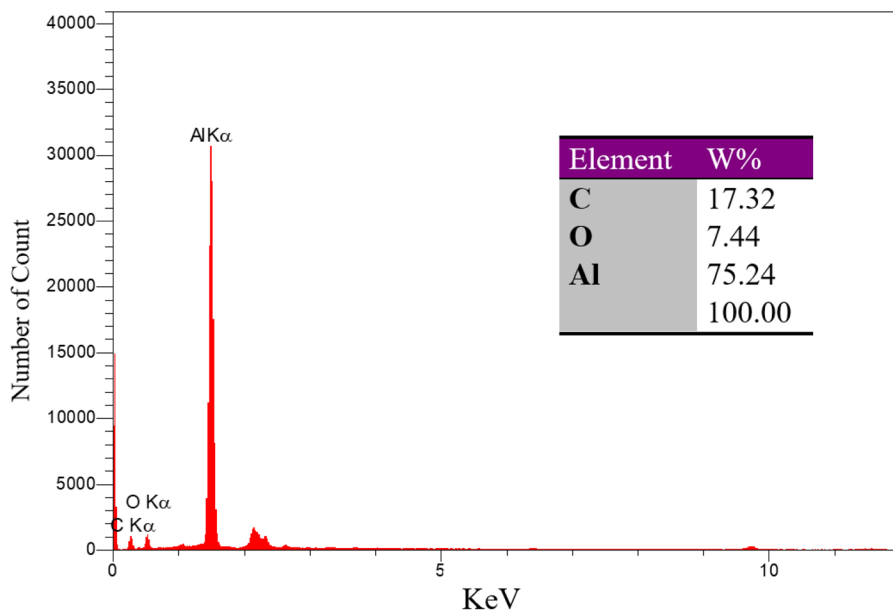
EDAX test results, as shown in Fig. 7a, showed the decoration of the constituents on the bacterial cell, which mainly contained Al,

O and C elements, confirming the absorption of nano alumina on the bacterial cell. These EDAX data were supported by FESEM to depict the decoration and actual cell permeability (Fig. 7b).

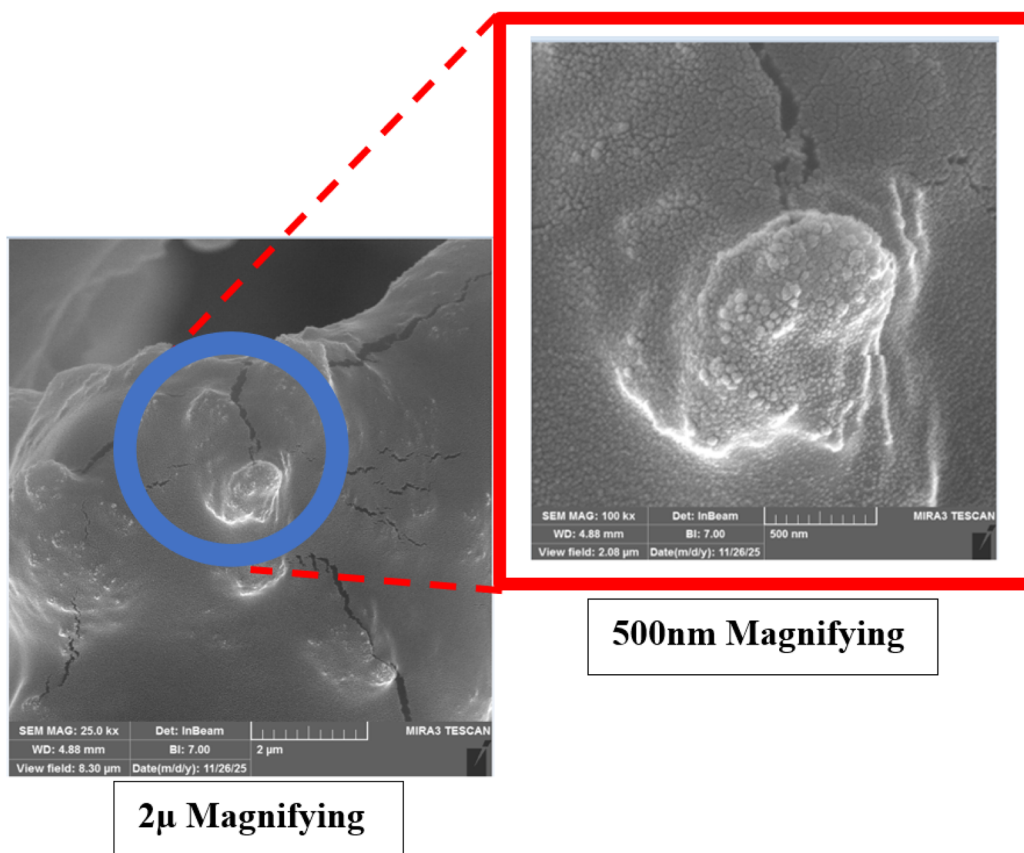
Viscosity

The results of viscosity measurements are shown in Table 3 and Fig. 8. After 12 days of upgrading, the viscosity reached its optimum, decreasing by over 50%. This result aligned with those of FTIR spectroscopy and GC-MS.





a



b

Fig. 7 (a) EDAX test and (b) FESEM depict the decoration of nano alumina on the bacterial cell surface.

Optimization

Based on quantitative FTIR spectroscopy and viscosity measurements across all 18 runs, the final results are

summarized in Table 3. Furthermore, ANOVA tables for both responses are shown through Tables 4 and 5. As shown in Fig. 9a–e, changes in the three variables clearly affected the



Table 3 Analyzed responses based on the measurements for 18 runs

Run	Factor 1	Factor 2	Factor 3	Response 1	Response 2
	Oil content (%V)	Upgrading time (day)	Nano (%W)	Aromatic/aliphatic index	Viscosity (cp)
Original oil	—	—	—	0.2319	480
Upgraded oil	—	14	—	—	200
Run 01	17	9	0.4	0.0768	150
Run 02	17	23	0.4	0.2222	250
Run 03	23	9	0.4	0.6674	154
Run 04	20	16	0.5	0.7343	135
Run 05	14	16	0.3	3.0360	135
Run 06	23	23	0.4	11.5034	260
Run 07	23	9	0.2	1.3679	210
Run 08	20	16	0.3	0.5629	137
Run 09	23	23	0.2	9.0053	149
Run 10	20	30	0.3	6.0484	270
Run 11	20	16	0.3	2.6846	137
Run 12	26	16	0.3	1.2471	139
Run 13	20	16	0.3	7.1333	137
Run 14	20	2	0.3	0.5910	460
Run 15	17	9	0.2	0.8964	208
Run 16	20	0.16	0.1	28.3894	140
Run 17	17	23	0.2	0.3084	149
Run 18	20	16	0.3	0.8980	200

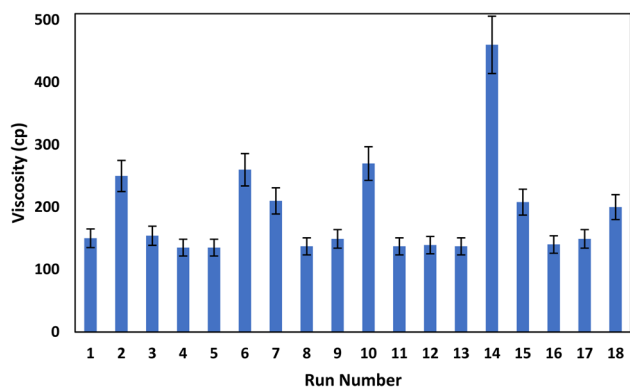


Fig. 8 Viscosity measurement for 18 experiment nanobioupgrading runs.

responses. The optimization was run to minimize both responses, in line with the research goals.

The ANOVA table for the first response (aromatic/aliphatic index) is shown in Table 4. The data were matched with a quadratic model. However, to validate the model and obtain a significant model, the terms AC (initial oil percent \times nano concentration) and B^2 (upgrading time) were crossed. Hence, the final modified quadratic model for the first response was:

$$\begin{aligned} \text{Aromatic/aliphatic index} = & + 50.39974 + 0.038953 \\ & \times \text{initial oil percent} - 2.20140 \\ & \times \text{upgrading time} - 211.61515 \\ & \times \text{nano concentration} + 0.11260 \\ & \times \text{oil} \times \text{time} + 0.70214 \times \text{time} \\ & \times \text{nano} - 0.036917 \times \text{oil}^2 \\ & + 277.28227 \times \text{nano}^2 \end{aligned} \quad (1)$$

The viscosity measurement in the final run (18) was outside the range of other data, and this run was a center point that replicated the same condition as runs 8, 11, and 13. Hence, the viscosity data from run 18 were removed to validate the model. The ANOVA table for the second response (viscosity) is shown in Table 5. The data were matched with a quadratic model. To validate the model and obtain a significant model, the terms AB (initial oil percentage \times upgrading time) and AC (initial oil percentage \times nano concentration) were crossed. Hence, the final modified quadratic model for the second response was:

$$\begin{aligned} \text{Viscosity} = & +486.77496 + 20.01042 \\ & \times \text{initial oil percent} - 54.41722 \\ & \times \text{upgrading time} - 619.56250 \\ & \times \text{nano concentration} + 58.12500 \\ & \times \text{upgrading time} \times \text{nano concentration} \\ & - 0.48750 \times \text{initial oil percent}^2 + 1.07372 \\ & \times \text{upgrading time}^2 - 426.25000 \\ & \times \text{nano concentration}^2 \end{aligned} \quad (2)$$

In Fig. 9a, for example, the higher oil volume maintained the aromatic/aliphatic index but also increased over time, unless for an upgrading time <16 days. Conversely, the lower oil volume had an acceptable aromatic/aliphatic range even for a long upgrading time, which may demonstrate the bacterial ability to metabolize low-volume oils. Fig. 9b–e show that the aromatic/aliphatic index for a higher initial oil volume could have remained low enough even by that time. This may be due to the higher concentration of nanoparticles (>0.1% W), which could be absorbed by the cell and intensify the upgrading process. However, this trend reached an optimum nano concentration of 0.4% W. The reason may be that after this concentration, the



Table 4 ANOVA table in Design Expert software for the first response (aromatic/aliphatic index)

Source	Sum of squares	Mean square	F-value	p-value probe > F	Validity	
Model	515.67	73.67	2.47	0.0949	Significant	
A-oil	19.06	19.06	0.64	0.4431		
B-t	52.37	52.37	1.75	0.2150		
C-nano	185.09	185.09	6.19	0.0321		
AB	44.73	44.73	1.50	0.2492		
BC	1.93	1.93	0.065	0.8044		
A ²	2.68	2.68	0.090	0.7707		
C ²	186.65	186.65	6.25	0.0315		
Residual	298.82	29.88				
Lack of fit	271.41	38.77	4.24	0.1312		Not significant
Pure error	27.41	9.14				
R-squared	0.6331					
Adj R-squared	0.3763					
Std. dev.	5.47					
Mean	4.19					

Table 5 ANOVA table in Design Expert software for the second response (viscosity)

Source	Sum of squares	Mean square	F-value	p-value probe > F	Validity	
Model	96 893.82	13 841.97	7.90	0.0021	Significant	
A-oil	37.52	37.52	0.021	0.8866		
B-t	5383.89	5383.89	3.07	0.1102		
C-nano	478.52	478.52	0.27	0.6127		
BC	13 243.78	13 243.78	7.56	0.0205		
A ²	420.00	420.00	0.24	0.6350		
B ²	60 394.37	60 394.37	34.46	0.0002		
C ²	396.41	396.41	0.23	0.6446		
Residual	17 525.42	1752.54				
Lack of fit	14 548.67	2078.38	2.09	0.2920		Not significant
Pure error	2976.75	992.25				
R-squared	0.8468					
Adj R-squared	0.7396					
Std. dev.	41.86					
Mean	190.03					

high-concentration nanoparticles could act as a barrier against the entrance of hydrocarbons through the cell. This mechanism could be improved by working on the initial oil concentration and nano concentration, besides the time. A lighter oil with a higher API degree could be more suitable for bacterial metabolism. Even for such a heavy oil, modified nanostructures (by applying a special coating) or using additives such as surfactants instead of increasing the nano concentration may improve the nanobioupgrading even slightly.

The optimization was summarized as an aromatic/aliphatic index of 0.07677, viscosity of 143.897 cp at a nano concentration of 0.46% W, upgrading time of 11.86 days, and oil volume percent of 26 %V. Based on the research objectives, the optimization goal was set on minimizing the upgraded oil viscosity and minimizing the aromatic/aliphatic index.

GC-MS analyses of upgraded crude oil

To analyze the structural changes in crude oil molecules in more detail, GS-MS for upgraded oils was run to assess the alteration of crude oil as per the 18 runs detailed in Table 6.

GC-MS allowed export of a sheet listing the identified compounds for each scan, with the maximum probability. Other GC-MS results showed the mass percentage of each compound relative to the total oil mass. Hence, with a known weight of each oil, the quantity of each compound was calculated in grams. As shown in Table 6, some heavy compounds in crude oil were completely transformed *via* nanobioupgrading. Most of these compounds were branched and cyclo compounds, which have a major role in heavy, viscous crude oils. For example, cyclo hydrocarbons such as 1R,2C,3 t,4t-Tetramethyl-cyclohexane, and Cyclohexane,1,1,3-trimethyl-were fully transformed and, conversely, the contents of some aliphatic hydrocarbons such as Eicosane increased. This means the bacteria could break chains and cyclo compounds. However, some unwanted transformation was observed in compounds such as 28-Nor-17.beta.(H)-hopane. This may have been related to the vaporization of volatile compounds and the decrease in bacterial activity during that time. The compounds cited in Table 6 played the part of donors.

These results aligned with the quantitative results of the FTIR spectra shown in Table 2. As shown in Table 6, cyclo



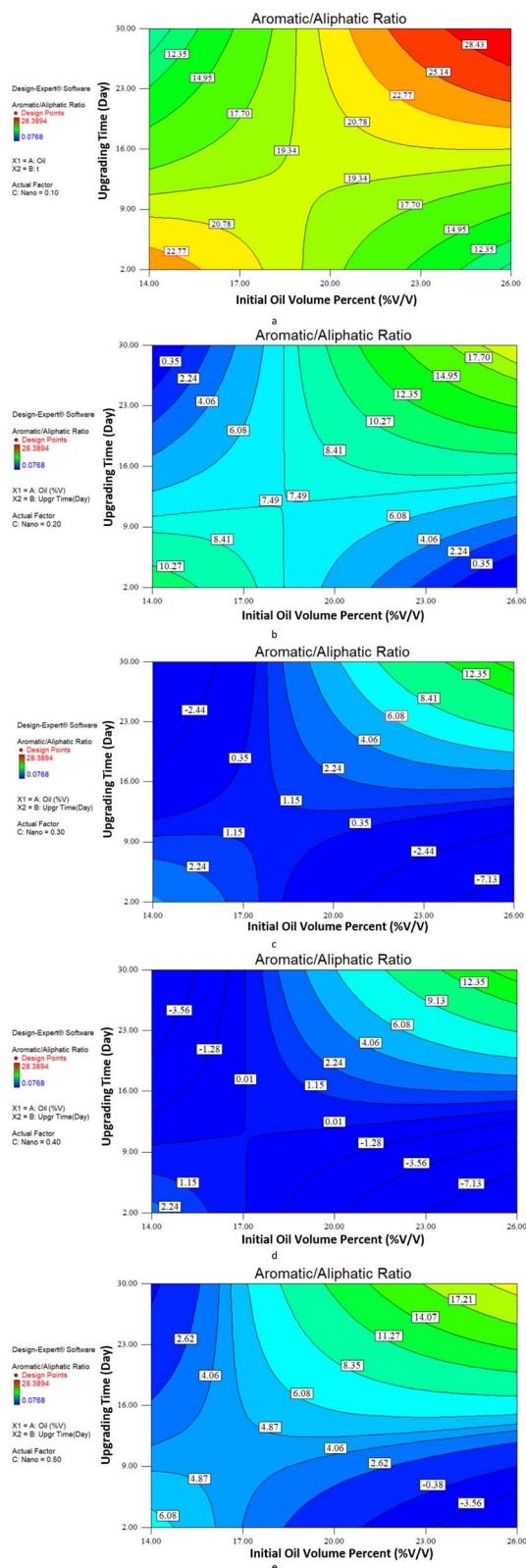


Fig. 9 Aromatic/aliphatic variation versus oil volume percent and upgrading time for (a) 0.1% W, (b) 0.2% W, (c) 0.3% W, (d) 0.4% W and (e) 0.5% W nanoparticle concentration.

compounds sharply decreased following nanobioupgrading during the first 2 weeks. However, a slight decrease was observed in branched aliphatic compounds. Conversely, aliphatic compounds increased during 12 days. Based on software-optimization results, 11.86 days would have been the optimal nanobioupgrading time during which bacteria could have maintained their metabolism as before. Furthermore, the chromatograms of GC-MS analysis for three statuses are shown in Fig. 10a-c: the original oil, bioupgraded oil and nano-bioupgraded oil at optimum conditions.

Nanobioupgrading efficiency (NBUE)

In the quantitative analysis of GC-MS results, key aliphatic and aromatic molecules were targeted to assess the nanobioupgrading capability of *G. stearothermophilus*.³⁸ The results are summarized in Table 6. As shown in the table, BE for most items was 100%. This means that *G. stearothermophilus* could have completely upgraded the crude oil in that fraction. Conversely, some fractions were increased in upgraded oils. This means these items were formed during the upgrade of the other fractions.

Based on the achieved results and literature review, a comprehensive analysis of the capability of *G. stearothermophilus* to bioupgrade heavy crude oil at high temperatures, focusing on the direct function of microorganisms, has not been done. Studies have mainly discussed the indirect role of bacteria in heavy oil upgrading through the production of their metabolites. However, in our research, the direct role of bacteria in upgrading by exposing heavy crude oil to bacterial cells was discussed. This achievement could be considered a key part of the novelty of our research, especially the type of applied bacteria: *G. stearothermophilus*. Previous studies have mainly applied other types of bacteria. Furthermore, another aspect of research novelty may be the combined and simultaneous application of bacteria and nanoparticles to show such direct application of bacterial cells in heavy oil upgrading. Other shortcomings in previous research may be the lack of investigations on reusing the bacterial medium to upgrade heavy crude oil. Hence, we investigated the capability of *G. stearothermophilus*. Our investigations confirmed the ability of microorganisms to use *n*-alkanes and other aliphatic hydrocarbons as a sole source of carbon, supported by the presence of multiple microsomal Cytochrome P450 enzyme systems. P450 enzymes catalyze the first step in alkane degradation, which is then processed by fatty alcohol oxidase and fatty aldehyde dehydrogenase, or by P450 monooxygenase, to yield fatty acids. We observed the same predicted pathway during heavy oil upgrading by water-soluble (hydrophilic) *G. stearothermophilus*. It means oxidation played a key part in upgrading pathways, such as the formation of hexyl-octyl ether.

The degradation pathway of cyclohexane under anaerobic conditions has been reported to be analogous to that of *n*-alkanes using glycol radical enzymes. The most common initial reaction during the anaerobic degradation of saturated and aromatic hydrocarbons, observed in several physiological types of anaerobes, is a radical reaction of hydrocarbons with fumarate, yielding substituted succinates.



Table 6 Nanobiougrading efficiency of *G. stearothermophilus* in terms of crude oil components

Compound	Prob%	Origin mass	Bio upgrading		Nano upgrading		Nanobio upgrading	
			Mass	E^a (%)	Mass	NE ^{a,d} (%)	Mass	NBUE ^b (%)
Heptane, 2-methyl-	81	1.525	0	100	0.305	80	0	100
Hexane, 1,1'-oxy bis-(dihexyl ether)	50	1.126	0	100	0	100	0	100
Hexane, 2,4-dimethyl-	95	3.408	0	100	0.341	90	0	100
Heptane, 2,6-dimethyl-	70	1.101	0	100	0.110	90	0	100
Cyclohexane, 1,1,3-trimethyl-	69	2.108	0	100	1.476	30	0	100
Nonane	69	5.438	0	100	0.544	90	0	100
Octane, 2,6-dimethyl-	82	2.773	0	100	0	100	0	100
Heptane, 3-ethyl-2-methyl-	85	0.758	0	100	0	100	0	100
1R,2C,3t,4t-Tetramethyl-cyclohexane	70	0.583	0	100	0.292	50	0	100
Nonane, 4-methyl-	85	0.702	0	100	0	100	0	100
Octane, 2,3-dimethyl-	78	5.246	0	100	0.525	90	0	100
Decane	95	1.630	0	100	0	100	0	100
Decane, 4-methyl-	74	0.795	0	100	0.040	95	0	100
Decane, 5-methyl-	54	0.425	0	100	0.021	95	0	100
Decane, 2-methyl-	96	0.826	0	100	0.041	95	0	100
Undecane	85	5.711	1.723	69.8	4.425	5	1.228	78.5
Hydroxylamine, O-decyl-	66	0.511	0	100	0	100	0	100
2,3-Dimethyldecane	58	0.590	0	100	0.059	90	0	100
Dodecane	83	5.355	0	100	0	100	0	100
Undecane, 2,6-dimethyl-	90	1.319	0	100	0.132	90	0	100
Tridecane	91	5.202	0	100	0	100	0	100
Dodecane, 2,6,10-trimethyl-	90	1.441	11.013	+86.9 ^c	0.288	80	11.013	+86.9 ^c
Heptadecane	80	4.841	0	100	0	100	0	100
Octadecane	74	3.522	0	100	0	100	0	100
Heptadecane, 2,6,10,15-tetramethyl-	93	3.549	0	100	0.710	80	0	100
Octadecane, 2-methyl-	45	2.702	0	100	0	100	0	100
Heptacosane	81	2.659	2.659	0	2.659	0	1.867	29.8
Octacosane	55	2.036	2.576	+21 ^c	1.629	20	2.576	+21 ^c
Tetratetracontane	65	1.912	0	100	0	100	0	100
Octadecane, 3-ethyl-5-(2-ethyl butyl)-	85	1.346	0	100	0	90	0	100
Nonadecane	78	4.760	4.760	0	4.760	0	3.613	24.1
Hexadecane	65	5.708	5.708	0	5.708	0	3.699	35.2
Tetradecane	70	4.922	3.399	30.9	4.430	10	3.401	30.9
Pentadecane	80	6.147	0	100	0	100	0	100

^a Quantitative analysis of results of GC-MS for biougraded crude oil after 14 days as the optimum time. ^b Quantitative analysis of results of GC-MS for nanobiougraded crude oil after 11.86 days as the optimum time. ^c The content of upgraded oil was increased. ^d NE (%) means control tests for nano-upgraded crude oil after 11.86 days, the optimum time (same condition as nanobiougrading).

RT-qPCR conducted by Tao *et al.* (2025) confirmed the crucial role of P450 monooxygenase in hydrocarbon upgrading.³⁹ They showed that P450 monooxygenase, along with other potential genes, AlkB-types, AlmaA-type, and LadA-type, are likely to have contributed to its high upgrading efficiency. Their investigation confirmed that P450 monooxygenase was strongly induced by C16 and C18, and weakly detected in the presence of C20–C28. Hence, this gene has a predominant role in the degradation of medium-chain alkanes (C16–C18). Aligned with quantitative analyses based on GC-MS results, P450 monooxygenase, which is typically associated with the oxidation of short and medium-chain alkanes, has a crucial role in the metabolism of hexadecane and octadecane.^{39,40} These results match GC-MS findings closely, as shown in Table 6. As shown in Table 6, the biougrading and NBUE of octadecane were 100%, indicating that, at both states, *G. stearothermophilus* alone and *G. stearothermophilus* and alumina nanoparticles together could strongly upgrade octadecane. This achievement may align with

the predominant enzyme identified in biougrading *via* RT-qPCR: P450 monooxygenase.

Here, the same analysis may be predominant. As per Table 6, the biougrading efficiency for hexadecane was zero, which means that bacteria could not metabolize it, or even that octadecane could not have entered the bacterial cell. However, after alumina absorption on the cell surface and improvement of cell permeability, which may have led to the entry of hydrocarbons into the cell, the NBUE of hexadecane was 35%, indicating that the probable pathway may have operated to some extent.

The rows 6, 12, 16, 19, 21, 23, 24, 27, 28, 29, 31, 32, 33 and 34 in Table 3 are normal alkanes with a different number of carbon atoms, which have been transformed based on GC-MS results. As shown in Table 6, based on calculations, the content of some components in the upgraded oil decreased, such as nonane and decane, while the content of others increased during the upgrading process, such as octacosane. The important note here is that the high viscosity of heavy crude oil was not solely



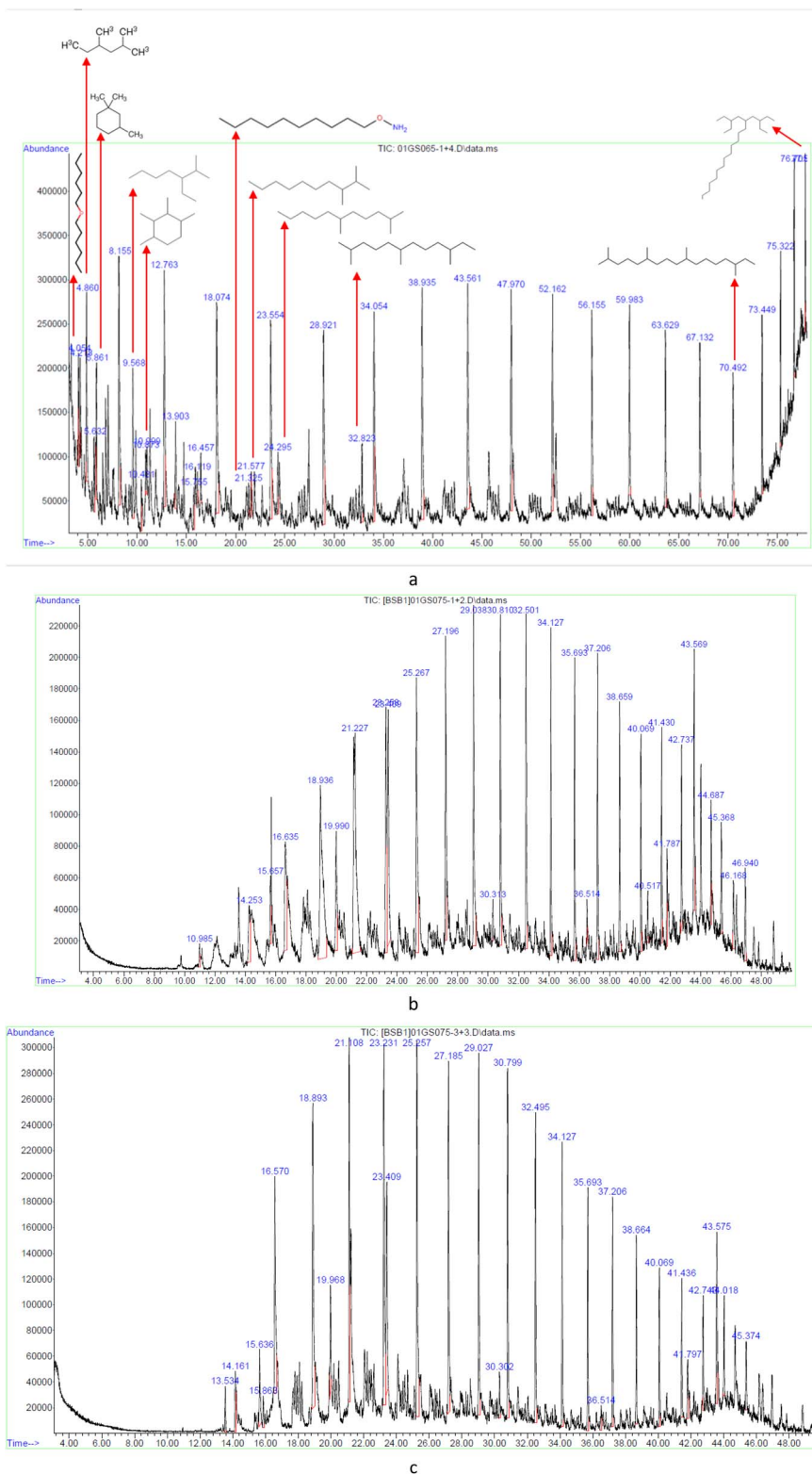


Fig. 10 GC-MS chromatogram for (a) original oil, (b) biougrading, and (c) nanobiougrading at optimum conditions.

due to heavy aromatic and asphaltene molecules; long-chain saturates may also have an important role in the high viscosity of heavy oils. This aligns exactly with the GC-MS results in Table 6. The same behavior was observed for the

biodegradation mechanism: anaerobic degradation of cyclohexane and anaerobic degradation of saturated and aromatic hydrocarbons. It is clear from rows 5 and 9 of Table 6 for cyclic molecules that Cyclohexane, 1,1,3-trimethyl- and 1R,2c,3 t,4t-



Table 7 Quantitative analysis of crude oil during control tests at optimum conditions

Run	Aromaticity index	Aliphatic index	Viscosity (cp)
Original oil at 25 °C	0.1678	0.7236	480
Oil at 60 °C in shaker (without nano and bacteria)	0.1670	0.7233	470
Exposed oil just to bacteria	0.1586	0.7539	450
Exposed oil just to nano alumina	0.1767	0.7299	460

Tetramethyl-cyclohexane have been completely upgraded. Regarding the above explanation, the transformation of hydrocarbons through nanobiougrading can be confirmed. Further to the control GC-MS tests, which are shown in Table 6, the results of control viscosity and FTIR spectroscopy, which are shown in Table 7, confirmed the synergetic effect of simultaneous use of bacteria and nanoparticles.

The other control laboratory experiments were run under the same experimental conditions, without any microorganism solution, and the tests were run only in the presence of nanoparticles. The results are shown in Table 7. As per results, the solo effect of bacteria and nanoparticles was not considerable, and this proved the synergetic effect of simultaneous use of bacteria and nanoparticles.

The adsorption of nano alumina to a bacterial cell surface can disrupt the impermeable surface of the cell, making it more permeable.⁴¹ This process could have facilitated the entry of hydrocarbons into the bacterial cell, and the bacteria used the heavy molecules as the sole source of carbon in the medium. In line with this analysis, nominated microorganisms may be enriched in biofilms complexed to the Al_2O_3 surface. The increased abundance of their carbohydrate and energy metabolism genes confirmed that EPS in an electron-deficient state accelerated the metabolism of external hydrocarbon substrates and energy by microorganisms.⁴² Vacancies in the Al_2O_3 structure complexed with EPS led to the absence of electrons in the biofilm, and a charge non-equilibrium state formed between EPS and the microorganism. Hence, the microorganism accelerated the acquisition of external electrons to maintain homeostasis.

This fact may intensify the permeability improvement of the bacterial cell surface, leading to greater entry of heavy oil molecules into the cell for metabolism by the bacteria. In fact, many efficient *G. stearothermophilus* were found to be enriched on the surface of Al_2O_3 . This phenomenon enhanced the intracellular metabolism of substrates and energy of PTS transmembrane proteins, promoted photosynthetic heterotrophy, and increased the rate of microbial upgrading of heavy oil molecules. The complexation of aluminum vacancies in the Al_2O_3 structure with EPS disrupted the electron balance of the biofilm and accelerated the acquisition of exogenous electrons by microorganisms without the addition of external energy.⁴² The probable biosorption of metal oxide nanoparticles may fall within six main categories: ion exchange, complexation, precipitation, physical adsorption, reduction, and chelation.⁴³ It seems alumina nanoparticles could have been absorbed by the bacterial cell through a combination of two or more of the

abovementioned mechanisms. Biosorption is a process in which biological materials concentrate organic or inorganic species dissolved in aqueous solutions (e.g., metals). This process uses passive physicochemical mechanisms based on the affinity between biomass cells (adsorbent) and metal ions (adsorbate) to be removed and the difference in concentration between the liquid phase and solid phase. Alumina absorption on the *G. stearothermophilus* surface may be strengthened by the presence of compounds on the bacterial cell surface, such as carboxyl, amino, and sulfonate groups. The negative surface charge of Gram-positive bacteria such as *G. stearothermophilus* is primarily due to compounds such as carboxyl, amino, and sulfonate groups. A schematic of ion interaction between alumina and the *G. stearothermophilus* cell surface is shown in Fig. 11.

This research achievement aligns with the pre-run SARA test in the pre-test, using only *G. stearothermophilus* without nanoparticles, as shown in Table 5. During pre-tests evaluating the

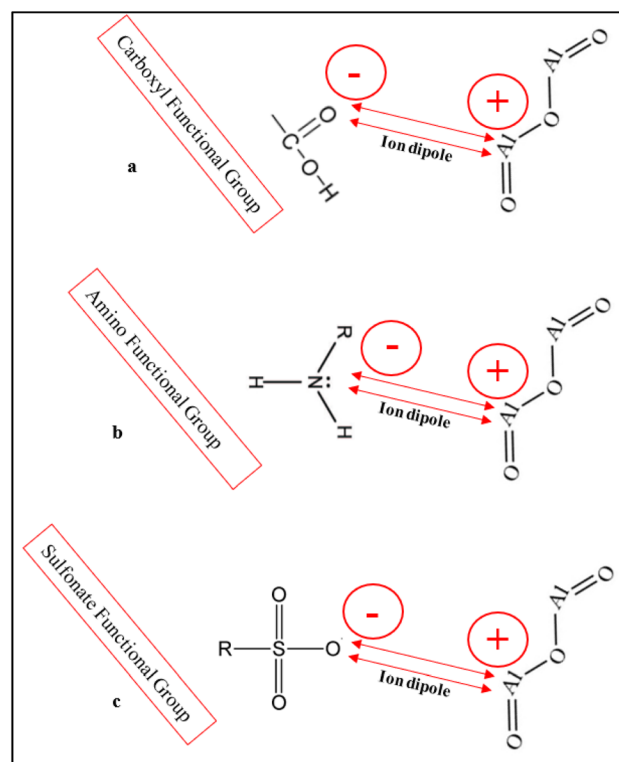


Fig. 11 Ion–dipole interaction between alumina nanoparticles and (a) carboxyl, (b) amino, and (c) sulfonate functional groups on the bacterial cell surface.



Table 8 SARA test results for the original oil and bioupgraded oil

Item	Compound	Saturate (%)	Aromatic (%)	Resin (%)	Asphaltene (%)
1	Original crude oil	47.9	28.10	14.9	9.10
2	Upgraded oil	69.10	12.90	13.80	4.20
3	Change percent %	44.26	54.09	7.38	53.85

function of *G. stearothermophilus* in upgrading before approaching the combined effect of bacteria and nanoparticles, a supplementary SARA test was conducted for the optimum upgraded oil after upgrading the oil by just *G. stearothermophilus* (at the optimum upgrading time of 14 days) to

facilitate a comparison between the original oil and upgraded oil. As shown in Table 8, an acceptable trend of upgrading was observed, indicating the function of the nominated bacteria. This achievement would be necessary to run the full set of SARA tests for nanobioupgrading samples in the future phase of the research.

As shown in Table 8, a sole bacterium could have increased the saturate contents and decreased the aromatic contents, which, combined with the nanobioupgrading test results, may confirm that the simultaneous effect of bacteria and nanoparticles could promote the upgrading of heavy oil.

The ability of *G. stearothermophilus* to tolerate high temperatures is mainly related to its enzyme production.^{44,45} Wang *et al.* showed that various heat-shock proteins, including DnaK,

Table 9 Comparison between previous studies and current research

Differences with current research		Research novelty versus the previous researches	Ref.
Research scope	Results		
- <i>Alcanivorax</i> , <i>Marinobacter</i> , <i>Thalassolituus</i> , <i>Cycloclasticus</i> and <i>Oleispira</i> bacteria as hydrocarbonoclastic bacteria	- Rapid degradation of many oil constituents	- Using <i>Geobacillus stearothermophilus</i> combined with nano alumina	
- No quantitative analysis	- Genome sequencing	- Fully quantitative analysis of bioconversion of crude oil fractions	
- Ambient temperature	- Potential of oil pollution mitigation	- Tests at 60 °C	
- No nano structures	- Potential of biopolymer production and biocatalysis	- Focus on upgrading (not only environmental concerns)	3
- Focus on pollutant removal (only environmental concerns)	- Saturates increased by 6% to 92%	- Using <i>Geobacillus stearothermophilus</i> combined with nano alumina	
- Using native microbial consortia (not a specific microorganism)	- Resins decreased by 10% to 70%	- Tests at 60 °C	
- No nanostructures	- Increase in the cyclic and branched alkanes	- Focus on upgrading (not only environmental concerns)	5
- Tests at 30 °C	- Decrease in the S & N compounds		
- Focus on pollutant removal (only environmental concerns)	- Maximum desulfurization rate of 40.6%	- Using <i>Geobacillus stearothermophilus</i> combined with nano alumina	
- Using <i>Pseudomonas</i>	- Cleavage of S-S bonds	- Tests at 60 °C	
- Just desulfurization	- 5 S-compounds were completely removed		7
- Tests at 30 °C	- Degradation of crude oil	- Using <i>Geobacillus stearothermophilus</i> combined with nano alumina	
- Using <i>Geobacillus stearothermophilus</i>	- Improved displacement efficiency	- Focus on the direct role of bacteria	
- Focus on the produced bioemulsion, not the direct role of bacteria	- Creating a favourable wettability	- Full analysis of bioconversion of crude oil fractions with a focus on aromatics and aliphatics	9
- No qualitative and quantitative analysis for crude oil bioconversion	- Improved mobility ratio	- Run the tests at a wide range of variables, upgrading time	
- Run the tests just in a short upgrading time	- -29.26% reduction in sulphur	- Using <i>Geobacillus stearothermophilus</i> combined with nano alumina	
- Catalytic aquathermolysis upgrading while steam injection (not eco-friendly)	- -21.27% decrease in resin	- Tests at 60 °C	
- Using copper/zinc/graphene oxide catalysts not microorganism	- -37.60% decrease in asphaltene		17
- Run the tests at extra high temp 320 °C	- -46.92% increase in saturates		
	- -66.48% reduction in oil viscosity		
	- -25.49% increase in API gravity		



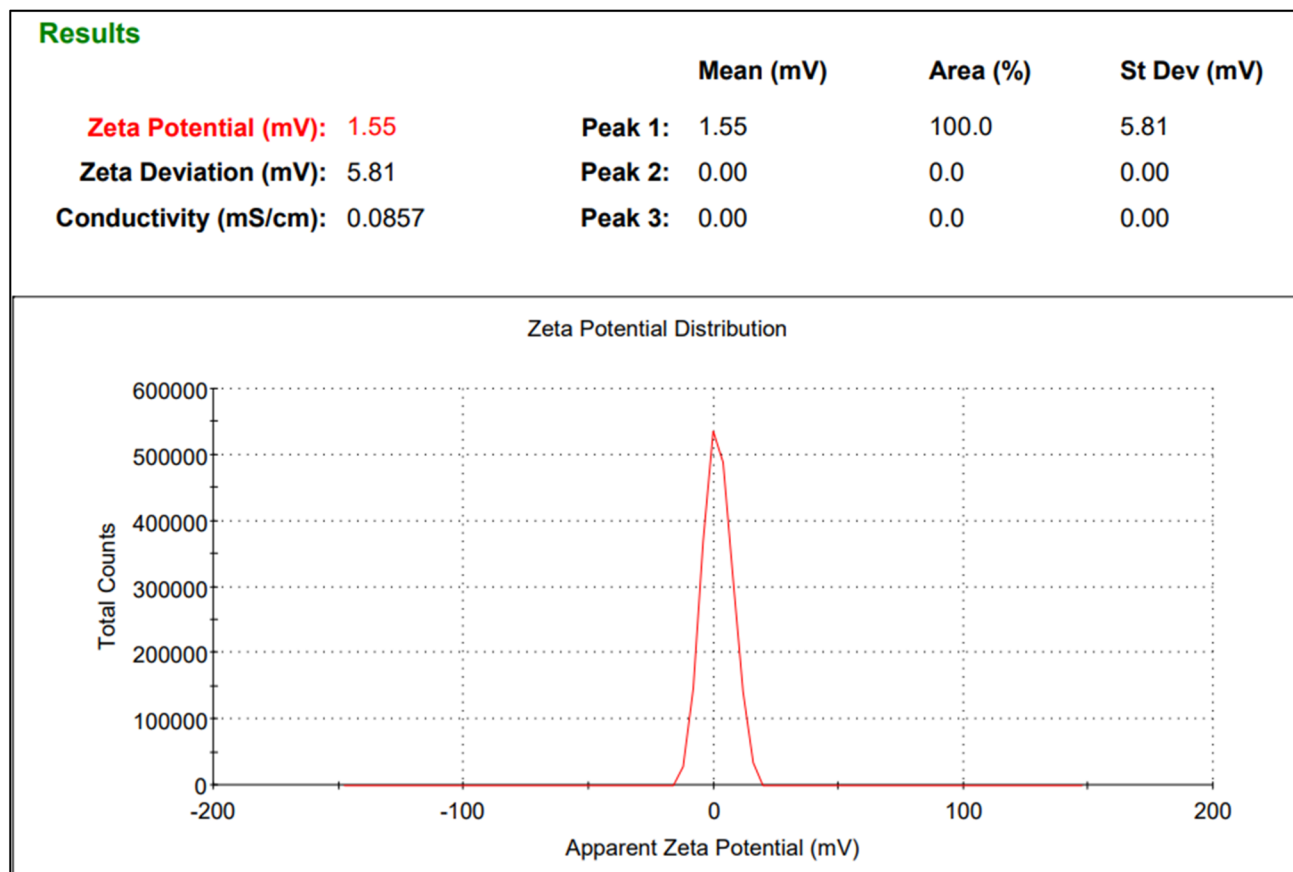


Fig. 12 The zeta potential confirmed the positive charge of nano alumina particles.

DnaJ, GrpE, GroEL, GroES, HSP33, and HSP20, may be responsible for such heat tolerance under harsh conditions.⁴⁴ However, environmental concerns regarding the use of Al₂O₃ nanoparticles may require greater attention to minimize environmental impacts during application through reservoirs.^{46–48} Due to the antibacterial effect of alumina nanoparticles, some harsh environmental impacts, such as retarding plant growth and increasing the mortality rate of organisms that depend upon it, should be considered, depending on exposure time and dose. However, although based on previous studies, the bioaccumulation and toxicity of nanoparticles increase with decreasing particle size, but the toxicity level is not alarming. Anyway, unprotected exposure to alumina nanoparticles should be avoided.⁴⁶

Finally, a quick comparison was run to depict the differences between previous studies and current research. The results are shown in Table 9. Furthermore, to confirm the purity and distribution of the constituents in the nanobacterial solution, an EDAX test was performed.

Zeta potential

As shown in Fig. 12, the zeta-potential results indicated a positive surface charge on alumina nanoparticles, consistent with the analysis shown in Fig. 11.

We wished to ascertain the nanobiouphgrading mechanism in more detail. Based on the FESEM data in Fig. 4, 5, 6 and 7,

dispersed alumina nanoparticles could have decorated the bacterial cell and adhered to the cell. This hypothesis was confirmed by the zeta-potential results, which revealed the positive charge of nano alumina, as shown in Fig. 12. Nano alumina could absorb heavy oil molecules and guide them into the bacterial cell.

G. stearothermophilus was intended to consume heavy oil molecules due to their inherent need for essential elements (C, O, S *etc.*), but such decoration by nano alumina could have intensified the metabolism.

Such interpretation aligns with the GC-MS results shown in Table 6, in which single biouphgrading could not have upgraded some fractions, such as heptacosane, nonadecane, and hexadecane. For undecane, upgrading efficiency was improved in the presence of nano alumina.

Conclusions

The present study highlights the nanobiouphgrading potential of combining *G. stearothermophilus* and alumina nanoparticles for the enhancement of heavy crude oil. This bacterial strain was chosen due to its considerable ability to metabolize crude oil compounds and its remarkable resilience in extreme temperatures in oil reservoirs. Alumina was chosen due to its nonpoisonous nature for bacteria and its capabilities in nanobiodesulfurization based on the literature. Upgrading



time, nanoparticle concentration, and the initial oil volume were considered the three independent variables at a fixed temperature of 60 °C. Aromatic/aliphatic content and oil viscosity were monitored as two independent responses in the experimental design using the bCCD method.

Outcomes were comprehensively analyzed using FTIR spectroscopy and GC-MS. Furthermore, for a thorough evaluation of our findings, we considered the mass percentage and calculated the NBUE based on GC-MS results across diverse samples. In addition, to quantitatively assess the results obtained from FTIR spectroscopy, we determined key indices for aliphatic and aromatic compounds during upgrading. The findings revealed that *G. stearothermophilus* could achieve 100% NBUE for upgrading aromatics and certain long-chain aliphatics over 11.86 days, which was identified as an optimal time period.

In terms of designed parameters at optimum conditions (11.86 days, 26% v/v initial oil, and 0.46% W nanoparticles), FTIR spectroscopy indicated a considerable reduction in the aromatic/aliphatic index from 0.29613 to 0.07677 and a decrease in oil viscosity from 480 cp to a maximum at 144 cp. GC-MS results showed a remarkable 100% decrease in certain contents. Also, asphaltene content was sharply reduced by 66%, resulting in a 14% improvement in decreased bacterial use.

These results hold substantial environmental importance due to the adverse effects associated with aromatics and the heavy constituents present in heavy crude oils. Also, reusing bacteria after separating them from upgraded oil samples was an important achievement in demonstrating the durability of their upgrading capacity. A notable advantage of using such bacteria is their natural occurrence in oil reservoir fluids. As a result, they are inherently adaptable to the conditions prevalent within oil reservoirs. Given their probable presence in oil reservoirs, there is no need for external colony injection. Notwithstanding, conducting field pilot tests to validate and optimize the proposed methodology is advisable. This step will ensure the practical viability and refine the implementation of this method. These findings highlight the synergistic efficacy of *G. stearothermophilus* and Al₂O₃ nanoparticles in upgrading heavy crude oil, offering a promising strategy for addressing energy demands. The results shed light on the simultaneous use of nanostructures and bacteria in heavy oil upgrading. At the field scale, growing bacteria in an isolated medium and making a nanobiological catalyst by nanostructures may have their own limitations and consequences. Future works may pay attention to the *in-situ* preparation of nanobiocatalysts in reservoir media by evaluating the wide range of nanostructures by focusing on local reservoir microorganisms. Finally, the potential application of such nanobioupgrading may be categorized as shown below.

- Improvement in exploitation and transportation

Such nanobiotechnology, by emphasizing the reduction in oil viscosity, may ease heavy oil exploitation through the well, transportation, and pumping through surface facilities to production units and refineries.

- Enhancement of oil recovery

The process may enhance oil recovery by decreasing oil viscosity and, consequently, improving oil mobility.

- Ease of refinery process

Due to improvements in heavy oil quality by reducing pollutant content, the refinery process may be simplified and streamlined. This research may shed light on the idea of subsurface refinery to improve the quality of oils at the subsurface.

- Environmental impacts

Due to the reduction and removal of pollutant content, environmental concerns are addressed, and the approach to a less-pollutant fuel becomes more accessible. Furthermore, such a method may be applied to remove soil and sea oil pollution.

Author contributions

Ali Maghzi: writing (original draft), data curation, data analyses, methodology, visualization. Arezou Jafari: conceptualization, review and editing, project administration, investigation, supervision. Seyed Mohammad Mousavi: conceptualization, review and editing, supervision. Riyaz Kharrat: conceptualization, review and editing.

Conflicts of interest

There are no conflicts to declare.

Data availability

The authors confirm that the data will be available upon request.

Acknowledgements

We thank the Department of Petroleum Engineering and Biotechnology at Tarbiat Modares University for their laboratory support during this research. Also, we appreciate the Research and Development Department of Petroleum Engineering & Development Company for their intellectual and financial support under contract number Pd-1401-7. In addition, this work is based upon research funded by Iran National Science Foundation (Grant number 4015535).

References

- 1 V. Leon and M. Kumar, *Biotechnol. Bioprocess Eng.*, 2005, **10**(6), 471–481.
- 2 W. A. Ismail, A. S. Raheem and D. Bahzad, in *Microbial Syntrophy-Mediated Eco-Enterprising*, Academic Press, 2022, pp. 125–175.
- 3 M. M. Yakimov, K. N. Timmis and P. N. Golyshin, *Curr. Opin. Biotechnol.*, 2007, **18**(3), 257–266.
- 4 M. Ghollami, M. Roayaei, F. Ghavipankeh and B. Rasekh, *J. Pet. Environ. Biotechnol.*, 2013, **4**(139), 1–5.
- 5 F. Ghaipankeh, Z. Ziaei Rad, J. Shayegan, M. Pazouki and A. Hosseinnia, *Adv. Environ. Technol.*, 2022, **8**(3), 215–228.
- 6 T. Tavassoli, S. M. Mousavi, S. A. Shojaosadati and H. Salehizadeh, *Fuel*, 2012, **93**, 142–148.



- 7 C. Ai, X. Zhang, S. Xue and P. P. Sun, *J. Environ. Chem. Eng.*, 2025, 118437.
- 8 J. F. Zhou, P. K. Gao, X. H. Dai, X. Y. Cui, H. M. Tian, J. J. Xie, G. Q. Li and T. Ma, *Int. Biodeterior. Biodegrad.*, 2018, **126**, 224–230.
- 9 H. Han, W. Zhu, Z. Song, K. Huang, H. Li and M. Yue, *Pet. Sci. Technol.*, 2020, **38**(6), 517–523.
- 10 C. Uzukwu and D. Dionisi, in *SPE Europec Featured at EAGE Conference and Exhibition*, SPE, 2016, pp. 180137.
- 11 E. Pandolfo, A. Barra Caracciolo and L. Rolando, *Water*, 2023, **15**(2), 375.
- 12 S. Irajli and S. Ayatollahi, *J. Pet. Explor. Prod. Technol.*, 2019, **9**(2), 1413–1422.
- 13 M. H. Shabani, A. Jafari, S. M. Mousavi and M. Abdi-Khanghah, *Energy Sources, Part A*, 2024, **46**(1), 15286–15296.
- 14 A. S. Raheem, D. Hentati, D. Bahzad, R. M. Abed and W. Ismail, *Int. Biodeterior. Biodegrad.*, 2022, **174**, 105468.
- 15 J. Zhang, *Energy*, 2023, **282**, 128863.
- 16 M. Abdi-Khanghah, A. Jafari, G. Ahmadi and A. Hemmati-Sarapardeh, *Energy*, 2023, **284**, 128267.
- 17 A. A. Soliman, M. E. Aboul-Fetouh, S. Gomaa, T. M. Aboul-Fotouh and A. M. Attia, *Sci. Rep.*, 2024, **14**(1), 25845.
- 18 J. Liu, S. Xiang, X. Zhou, S. Lin, K. Dong, Y. Liu, D. He, Y. Fan, Y. Liu, B. Xiong and K. Ma, *Lubricants*, 2025, **13**(7), 281.
- 19 Y. L. Liu, Y. Li, Y. F. Si, J. Fu, H. Dong, S. S. Sun, F. Zhang, Y. H. She and Z. Q. Zhang, *Energy*, 2023, **272**, 127123.
- 20 F. Ansari, P. Grigoriev, S. Libor, I. E. Tothill and J. J. Ramsden, *Biotechnol. Bioeng.*, 2009, **102**(5), 1505–1512.
- 21 T. Zhang, W. L. Li, X. X. Chen, H. Tang, Q. Li, J. M. Xing and H. Z. Liu, *World J. Microbiol. Biotechnol.*, 2011, **27**, 299–305.
- 22 Z. Tohidi, A. Teimouri, A. Jafari, R. Gharibshahi and M. R. Omidkhah, *J. Pet. Sci. Eng.*, 2022, **208**, 109602.
- 23 M. Hasani and A. Jafari, Electromagnetic field's effect on enhanced oil recovery using magnetic nanoparticles: Microfluidic experimental approach, *Fuel*, 2022, **307**, 121718.
- 24 S. Ahmady-Asbchin, M. Akbari Nasab and C. Gerente, Heavy metals biosorption in unary, binary, and ternary systems onto bacteria in a moving bed biofilm reactor, *Sci. Rep.*, 2024, **14**(1), 19168.
- 25 S. Xie, *Green Chem. Lett. Rev.*, 2024, **17**(1), 2357213.
- 26 Z. Chen, J. Li, J. Zhang, H. Wang, Y. Zeng, F. Wang, P. Huang, X. Chen, L. Ge, R. A. Dahlgren and H. Gao, *J. Cleaner Prod.*, 2024, **435**, 140497.
- 27 A. Mandal, E. Dhineshkumar and T. P. Sastry, *Clean Technol. Environ. Policy*, 2023, **25**(10), 3285–3302.
- 28 A. Mandal, M. Katheem Farhan and T. P. Sastry, *Clean Technol. Environ. Policy*, 2016, **18**(3), 765–773.
- 29 A. Mandal, E. Dhineshkumar and E. Murugan, *ACS Omega*, 2023, **8**(27), 24256–24267.
- 30 A. Mandal, A. Poongan, E. Dhineshkumar and E. Murugan, *ACS Appl. Eng. Mater.*, 2023, **1**(8), 2137–2152.
- 31 X. Li, P. Liu, Z. Wang, P. Liu, X. Wei, Y. Wu and T. Lei, *Renewable Energy*, 2025, **241**, 122368.
- 32 L. Guo, W. Chen, C. Wang and B. Dong, *Int. J. Electrochem. Sci.*, 2023, **18**(1), 26–32.
- 33 D. C. C. da Silva Medeiros, M. Usman, P. Chelme-Ayala and M. G. El-Din, *Energy Environ. Sustainability*, 2025, **1**(2), 100028.
- 34 Z. Li, D. Liao, G. Tian, X. Fan, X. Chai, W. Chang, Y. Gao, B. Yuan, Z. Li, F. Wei and C. Zhang, *J. Am. Chem. Soc.*, 2025, **147**(36), 32548–32559.
- 35 A. B. Mbouopda Poupi, K. Nchimi, R. Nguete, M. Iqbal, V. Poulouse, K. Sasaki and H. Saibi, *Pet. Sci. Technol.*, 2024, **42**(22), 3243–3263.
- 36 *Handbook of Hydrocarbon and Lipid Microbiology*, ed. Timmis, K. N., Springer, Berlin, 2010, vol. 552, p. 4716.
- 37 R. Rehman, M. I. Ali, N. Ali, M. Badshah, M. Iqbal, A. Jamal and Z. Huang, *J. Hazard. Mater.*, 2021, **418**, 126276.
- 38 I. Zojaji, A. Esfandiarian and J. Taheri-Shakib, *Adv. Colloid Interface Sci.*, 2021, **289**, 102314.
- 39 W. Tao, J. Lu, J. Lin, M. Ding, W. Wang and S. Li, *Ecotoxicol. Environ. Saf.*, 2025, **290**, 117780.
- 40 J. G. Speight and N. S. El-Gendy, *Introduction to Petroleum Biotechnology*, Gulf Professional Publishing, 2017.
- 41 *Applying Nanotechnology to the Desulfurization Process in Petroleum Engineering*, ed. Saleh, T. A., IGI global, 2015, pp.384–386.
- 42 H. Zhang, C. Hu, P. Zhang, T. Ren and W. Cai, *Sci. Total Environ.*, 2023, **904**, 166596.
- 43 H. P. de Sa Costa, M. G. C. da Silva and M. G. A. Vieira, *J. Water Process Eng.*, 2021, **40**, 101925.
- 44 J. Wang, W. Wang, H. Wang, F. Yuan, Z. Xu, K. Yang, Z. Li, Y. Chen and K. Fan, *Appl. Microbiol. Biotechnol.*, 2019, **103**, 4455–4465.
- 45 M. H. Wells-Bennik, P. W. Janssen, V. Klaus, C. Yang, M. H. Zwietering and H. M. Den Besten, *Int. J. Food Microbiol.*, 2019, **291**, 161–172.
- 46 N. A. Ogolo and M. O. Onyekonwu, *Arabian J. Chem. Environ. Res.*, 2021, **8**, 247–258.
- 47 E. A. Kumah, R. D. Fopa, S. Harati, P. Boadu, F. V. Zohoori and T. Pak, *BMC Public Health*, 2023, **23**(1), 1059.
- 48 N. Doskocz, K. Affek, M. Matczuk, M. Drozd and M. Załęska-Radziwiłł, *Desalin. Water Treat.*, 2025, **321**, 100988.

